Reduced Multiuser-Interference for Vehicular VLC using SDMA and Matrix Headlights

Claas Tebruegge*†, Agon Memedi*, Falko Dressler*
*Heinz Nixdorf Institute and Dept. of Computer Science, Paderborn University, Germany
†HELLA GmbH & Co. KGaA, Lippstadt, Germany
{tebruegge,memedi,dressler}@ccs-labs.org

***Abstract*—We investigate a novel approach of utilizing modern Adaptive Front-Lighting System (AFS) to reduce multiuser interference in Vehicular Visible Light Communications (V-VLC) by applying Space-Division Multiple Access (SDMA). V-VLC is a promising technology that can complement Radio Frequency (RF) communications to fulfill the high reliability and low latency requirements of Intelligent Transportation Systems (ITS). To achieve this, however, limitations of bandwidth efficiency and multiuser interference need to be addressed. A possible solution is to take advantage of SDMA, which allows spatial reuse of the resources and a simple but efficient multiple access method. State-of-the-art AFS, consisting of multiple controllable Light Emitting Diodes (LEDs) with sharply separated radiation patterns, offer a great opportunity to implement SDMA. Therefore, we investigate the applicability of an AFS-based SDMA system for V-VLC and compare its communication performance with a common LED-based high beam. Simulation results show that our system can be used to reduce multiuser interference in V-VLC.**

I. Introduction

Although technological advances in the automotive industry have contributed in the decline of fatalities on roads, traffic accidents remain one of the leading causes of death.[1] To counteract this, researchers, governments, and international institutions have promoted the development of Intelligent Transportation Systems (ITS). ITS suggest the use of communication technologies to enable information exchange between vehicles and infrastructure [1], [2]. By means of communication, vehicles can share relevant information to enable ITS applications (e.g., platooning, cooperative awareness) that improve safety and efficiency on roads.

Radio technologies like Dedicated Short Range Communication (DSRC) [3] and Cellular Vehicle-to-Everything (C-V2X) [4], have already been considered for vehicular networking. However, due to issues with inter-node interference [5] and high latency, these technologies might fall short in supporting safety-related applications, which have stringent requirements with respect to reliability metrics [6].

A potential solution for this is the combined use of multiple communication technologies, in particular, Line Of Sight (LOS) technologies, like Visible Light Communications (VLC) and Millimeter Wave (mmWave), which can easily overcome scalability issues. Here, VLC provides a license-free spectrum, low implementation cost and improved security against jamming and man-in-the-middle attacks.

VLC is a novel communication technology enabled by the fast switching capability of Light Emitting Diodes (LEDs). The superior lighting and environmental characteristics of LEDs has bolstered their adoption as the favorite source of illumination in indoor and outdoor setups, therefore making VLC available too. VLC-enabling front-ends for indoor use are available in the market, and have already been adopted in buildings[2]. For outdoor use, the progress has been somewhat slower due to the challenging conditions imposed by bad weather, sunlight, and other disturbances. On the other hand, Vehicular Visible Light Communications (V-VLC) has emerged as a promising application for outdoor VLC [7].

V-VLC is based on the use of modern LED-based headlights and taillights in vehicles for data communication. Important aspects of V-VLC are directly impacted by the technology used in exterior lighting modules and regulations from the automotive domain which apply to them. For instance, the low pass behavior of the LEDs installed in modern headlights and taillights limits the maximum achievable bandwidth [8], whereas safety regulations which define the shape and luminous intensity of the radiation patterns [9] impact the signal strength [10], [11]. Such limitations require the design of efficient communication schemes which can maximally exploit the available resources. One possibility is to take advantage of Spatial Multiplexing (SM) and beamforming.

Recent advancements in exterior automotive lighting technology have resulted in the development of advanced Adaptive Front-Lighting System (AFS), among others. Modern state-of-the-art AFS are implemented as an array (or matrix) of LEDs co-located within a lighting module. The physical separation of individual LEDs, their sharply separated radiation beams, and the ability to independently control each one of them allows the use of SM techniques for V-VLC. As a result, by means of spatial reuse of the resources we can drastically increase the communication efficiency.

In this paper, for the first time, we conceptually demonstrate Spatial Multiplexing for an AFS consisting of an high-end matrix LED headlight. Besides improved communication efficiency, through Space-Division Multiple Access (SDMA) we are also able to address multiuser interference by using

[1]World Health Organization, "Global status report on road safety 2018," 2018. https://apps.who.int/iris/bitstream/handle/10665/276462/9789241565684-eng.pdf

[2]www.purelifi.com/case-studies/

multiple physical channels. This allows simplification of higher layer protocols, resulting in reduced overhead and latency.

Our main contributions can be summarized as follows:

- We developed a concept to implement SDMA based on AFS which optimizes signal strength while maintaining low multiuser interference;
- using realistic optical simulations, we show the decrease in multiuser interference for our setup compared to traditional LED-headlights; and
- we thoroughly investigated the impact of our system on communication performance.

II. Related Work

The use of multiple transmitters and multiple receivers has already been considered in the V-VLC domain. Luo et al. [12] study the increase in bandwidth efficiency when using two headlights and two Photodiodes (PDs) for car-to-car communication. The authors use a comprehensive analytical model which considers LOS and Non LOS (NLOS) links (assuming road reflections with Lambertian profile), and channel disturbances (i.e., thermal noise and shot noise). Monte Carlo simulation results show that, for certain PD mounting heights, the communication up to 40 m is possible with a data rate of 40 Mbit/s.

In [13], Turan et. al take advantage of transmitter diversity to improve communication reliability. They use two fog lights to transmit the same signal and a PD on the receiving side. Results based on real-world measurements show an increased Packet Delivery Ratio (PDR) for short communication distances, and degradation for larger distances due to mutual interference.

In another empirical study, Narmanlioglu et al. [14] investigate the feasibility of Multiple-Input Multiple-Output (MIMO) based on multiple LED taillights and PDs installed close to the headlights of the following vehicle. Bit Error Rate (BER) curves from various MIMO modes show that SM provides better communication performance, whereas, regarding transmitter configurations, Signal-to-Noise Ratio (SNR) suffers due to power division when all of the taillights are used concurrently.

The aforementioned approaches are based on using PDs as receivers. However, V-VLC MIMO can also be realized when using camera image sensors on the receiving side [15]. In such cases, instead of using multiple receivers, image processing techniques are used to distinguish the spatially separated transmitters in images captured by the receiver [16]. Goto et al. [17] have demonstrated the feasibility of such a system, using a 4x5 LED array (where each LED transmits the same optical-OFDM signal) and a specially designed high-rate optical communication image sensor. One drawback of this system is the high price of the custom receiver. Nevertheless, in a controlled lab environment the presented system achieves a data rate of 54 Mbit/s.

In a similar study, a low frequency camera has been used to implement a 3x3 MIMO system based on the different wavelengths of a single RGB LED, rather than spatial separation on the transmitting side [18]. Such a system could be implemented for V-VLC, however, RGB LEDs are not used for exterior automotive lighting.

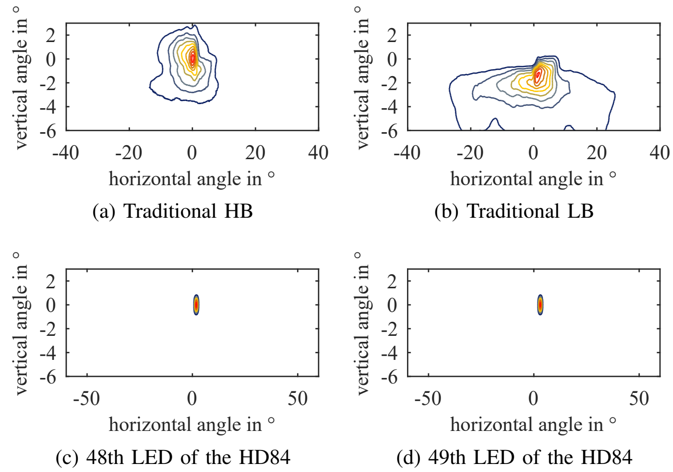

Figure 1. Isocandala pattern of different headlights; the red and blue colors represent high and low luminous intensities respectively

Recently, we also presented a novel receiver-based interference reduction mechanism using a spatial light modulator in form of a Liquid Crystal (LC)-panel to spatially filter interference and ambient light and to reduce interference to a minimum [19].

While, all of the above studies focus on bandwidth efficiency improvements by means of MIMO, in our study we also consider the benefits in terms of multiuser interference reduction. Additionally, we perform SM in LED level, which is more fine grained than using a separate lighting module as it is done in [13], [14].

III. Spatial Multiplexing with Matrix Headlights

LED technology has had a huge impact on automotive lighting in recent years. LEDs are more efficient, enable very bright light from small spaces and are robust enough to last more than a vehicle's lifetime. Because LEDs can be controlled quickly and specifically, adaptive headlamps are possible which illuminate an optimum area depending on the driving situation. Among other things, glare-free high beams are even possible, where the high beam can be turned on even if other traffic participants are around by specifically dimming the corresponding LED which points to the participant.

The HELLA HD84 is one of the most advanced of these headlamps. With 84 individually controllable LEDs, there is a very high degree of freedom in the choice of illumination. In Figure 1, we show the isocandela pattern of a traditional HB, a traditional LB, and two neighboring LEDs of the HD84. The isocandela patterns describe how much luminous intensity is radiated in which angle, while the red color means high intensity and the blue color means low intensity. A traditional HB has the highest intensity in the center for positive and negative vertical angles around the horizon (0 degree line). In contrast, the LB has high intensity only in negative vertical angles and a strong asymmetry in horizontal angles. In order not to glare oncoming traffic, high intensities can only be

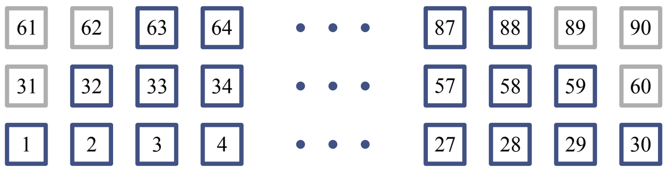

Figure 2. Arrangement and the corresponding ID of the HD84 Matrix LEDs

observed with a very small vertical angle in the left side of the isocanelda pattern. The HD84 can be separated in 84 single radiation patterns which correspond to a single LED each. As shown in Figure 1, the isocandela patterns have narrow spots of high intensity, thus, each single LED corresponds to a very small angle or area. So, signals can be emitted in a very targeted manner.

The arrangement of these LEDs is shown schematically in Figure 2. LED 1 illuminates the lower left area while LED 30 illuminates the lower right area. The second and third row starting with LED 32 and LED 63, respectively, illuminate larger vertical angles. The remaining LEDs (grayed out in Figure 2) are not used for high and low beam, respectively.

In communication technology, SM is one key to further increase bandwidth efficiency. By introducing multiple antennas or even antenna arrays, the direction of radiation can be controlled. Thus, resources in time and frequency domain can be spatially reused and multiuser interference can be prevented efficiently. Generally SM is very attractive for visible light communication due to the directivity of light and the straightforward implementation by using multiple LEDs. Through the use of suitable optics a very sharp and freely designable beam shape can be achieved, which can offer a lower spatial channel correlation.

The requirements for optical SM harmonize well with the requirements of modern LED Matrix headlights. The beams of single LEDs are sharply separated from each other in order to independently dimm the LEDs and selectively avoid glaring. Thus, in V-VLC, this effect is even stronger due to the special optical design of matrix headlights. Different to RF communication, the Matrix-V-VLC channel can be modeled simply due to the dominant LOS component and the sharp separation of beams, especially in the horizontal axis. This provides the ability to accurately predict and select the best channel without continuous Channel State Information (CSI), but with position information of Transmitter (TX) and Receiver (RX). Such position information can be made available in the case of vehicular application either by sensors like RADAR, LiDAR, cameras, or by the communication itself.

IV. Controlling the LED Matrix

For a reliable matrix communication, it is crucial to pick the optimal LED to be modulated with the signal. We propose to choose the LED that generates the highest received power at the transmitter. In the following, this LED is called *optimal LED*. Therefore, a camera system in the front of the car detects the scenario, classifies objects like cars and provide the positions to a controller. For this purpose the light source detection system

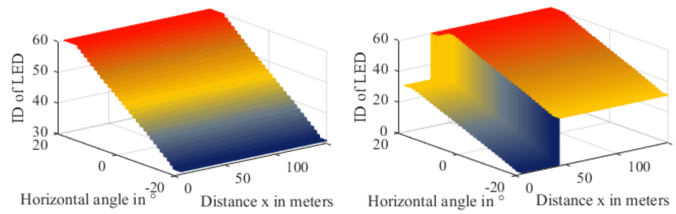

(a) PD and light source at same hight (b) light source 45 cm higher than PD

Figure 3. Optimal LED in dependence of angle and distance.

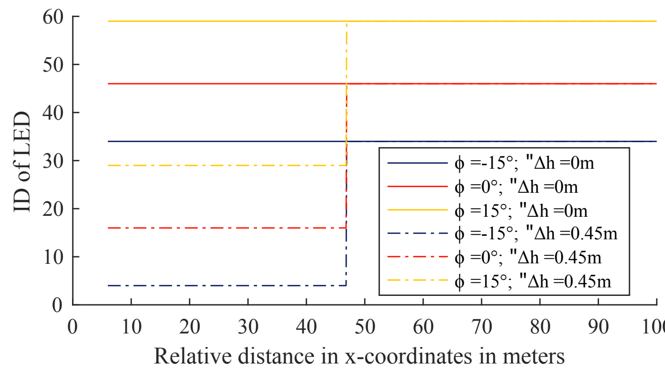

Figure 4. Optimal LED depending on angle and distance for different heights between RX and TX.

of HELLA Aglaia Mobile Vision GmbH was used, which is usually implemented in vehicles with AFS, so this concept can save overhead in comparison to systems where the Received Signal Strength (RSS) is fed back to the TX. The controller selects the optimal LED to be modulated with the signal.

To determine the optimal LED, in a pre-processing step, we can determine the LED with the strongest signal by finding the highest luminous intensity of the light distribution for each relative position. In Figure 3 the LED with the highest luminous intensity is shown over the relative angle of RX and TX and the relative distance. The dependency is rather simple, if TX and RX are at the same height. There, the choice of the optimal LED depends only on the angle between TX and RX. This behavior is shown in Figure 3a, in which the number of the optimal LED is plotted over the vertical angle and the distance.

If there is a height difference, also the distance has an influence on the optimal LED as shown in Figure 3b. For example, for a height difference of $\Delta h = 45\,\mathrm{cm}$, which occurs for a headlight at 65 cm and a RX at the minimum allowed height of a license plate (20 cm). This results in the following behavior. For close distances, less than 46.9 m, the first row offers more signal strength. Starting from 46.9 m distance, the optimal LED behaves same for $\Delta h = 45\,\mathrm{cm}$ and TX and RX at the same height, as shown in Figure 4.

A controller for choosing the optimal LED can be implemented as follows: by realizing a lookup table based on pre-processed position data; or, depending on memory constraints of the controller, using a simple linear function to choose the optimal LED. If RX and TX are on the same height, the optimal LED for the HD84 can be mapped precisely as (cf.

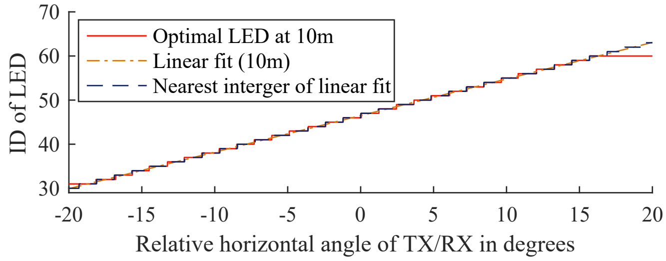

Figure 5. Angular dependency of the optimal LED at a distance of 10 m.

Figure 5)

$$\text{LED} = \begin{cases} 32 & \text{for } \phi < -19^\circ \\ \lfloor 0.829 \times \phi + 46.498 \rceil & \text{for } -19^\circ \leq \phi \leq 16.5^\circ \\ 59 & \text{for } \phi > 16.5^\circ \end{cases} . \quad (1)$$

Equation (1) consists of three parts: small angles are mapped to the leftmost LED (32), large angles are mapped to the rightmost LED (59), in between a linear function is applied.

We empirically mapped the values based on our measurements. Figure 3b gives an impression of the necessary step function in terms of selecting different rows of the matrix headlight if TX and RX are at different heights. Again, this can be implemented by lookup tables or a proper fitting function. Of course, height differences can be bridged by simply choosing full columns of LEDs instead of single LEDs.

V. Evaluation

The performance gain of SDMA using matrix headlights is investigated by comparing the photometric radiation patterns, the resulting signal strengths and BER by utilizing geometric dependencies and specifications of real components. This model was introduced in [11]. In this case the parameters shown in Table I are applied. The light distributions were simulated using ray-trace based optical simulations. For the optical simulation of the HD84, about 25 million rays have been simulated. Because of the finite number of rays, areas of very low illumination appear to have a signal strength of zero, however, we can assume these areas will be non-zero, but still with very low illumination or signal strength.

A. Channel Matrix for a Static Two Lane Scenario

We used P-matrices to assess the performance of using matrix headlights for SM. They include the received power for

Table I
Simulation parameters.

TX height	65 cm
RX height	65 cm
PD type	Thorlabs PDA100A
PD active area	10 mm × 10 mm
PD gain	0.75×10^3 V/A
Bandwidth	2 MHz
Illuminance of the sun	100 klx
Thermal noise	−58.893 dBm
Rays in optical simulation	25 484 095

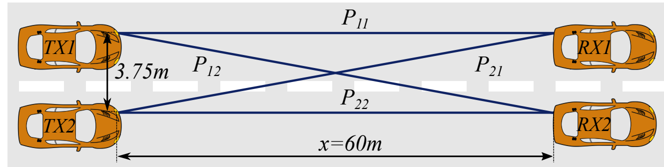

Figure 6. Two lane scenario.

different links between vehicles as

$$\boldsymbol{P} = \begin{bmatrix} P_{11} & P_{12} \\ P_{21} & P_{22} \end{bmatrix} . \quad (2)$$

P_{11} and P_{22} consist of the link between two cars on the same lane. P_{12} describes the link to the car one line on the right, while P_{21} describe the link to a car one lane to the left. The cars driving in the middle of the 3.75 m wide lanes, with a distance to preceding vehicle of 60 m, as it is shown in Figure 6. A high value of P_{ij} means that there is a strong signal strength at corresponding target. If all other values are small this means there is a low interference to other traffic participants.

For the HB with the matrix $\boldsymbol{P_{HB}}$ (cf. Equation (7)), the diagonal of the matrix contains the highest values, so the car on the same lane will receive the strongest signal. The cars on the left and the right lane receive around 10 dB less signal strength. The HB is not adaptive, so it can not be further controlled, which means this relation can not be changed. However, the matrix LED headlight can be controlled. For comparison LED 46, 44, and 49 are investigated: LED 46 has a strong component on the diagonal but very low values besides, cf. Equation (3). This means it can communicate well with the same lane car without interfering the others. LED 44 has a strong P_{12} and LED 49 has a strong P_{21} component, which enable a strong link to the right or left lane vehicle, respectively, cf. Equations (4) and (5). At the same time all other components containing much smaller values (at least 79 dB less), which decrease multiuser interference to the noise floor.

$$\boldsymbol{P_{46}} = \begin{bmatrix} -39.9\,\text{dBm} & 0 \\ -126.8\,\text{dBm} & -39.9\,\text{dBm} \end{bmatrix} \quad (3)$$

$$\boldsymbol{P_{44}} = \begin{bmatrix} -120.7\,\text{dBm} & -137.3\,\text{dBm} \\ -39.7\,\text{dBm} & -120.7\,\text{dBm} \end{bmatrix} \quad (4)$$

$$\boldsymbol{P_{49}} = \begin{bmatrix} -126.8\,\text{dBm} & -39.5\,\text{dBm} \\ -118.5\,\text{dBm} & -126.8\,\text{dBm} \end{bmatrix} \quad (5)$$

$$\boldsymbol{P_{LB}} = \begin{bmatrix} -88\,\text{dBm} & -54.2\,\text{dBm} \\ -88.9\,\text{dBm} & -88\,\text{dBm} \end{bmatrix} \quad (6)$$

$$\boldsymbol{P_{HB}} = \begin{bmatrix} -41\,\text{dBm} & -53.7\,\text{dBm} \\ -47.2\,\text{dBm} & -41\,\text{dBm} \end{bmatrix} \quad (7)$$

B. Dynamic Two Lane Scenario

To evaluate the effect on the V-VLC communication link, we use again the scenario shown in Figure 6. This time, we vary the distance x. The vehicle TX2 is transmitting to RX1 while RX2 gets interfered by this transmission. To investigate this scenario,

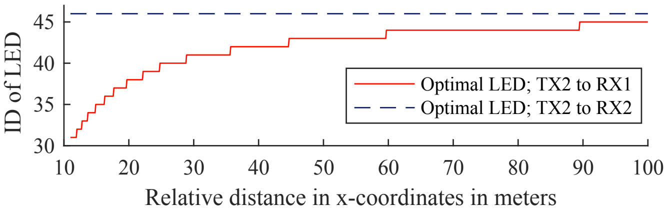

Figure 7. The optimal LED for the dynamic two lane scenario.

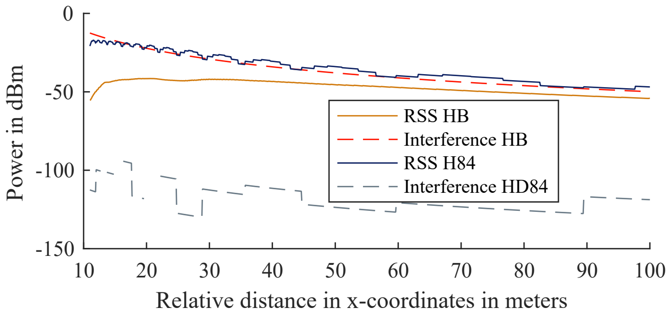

Figure 8. Signal and interference power of the HB of HD84 in the two lane scenario.

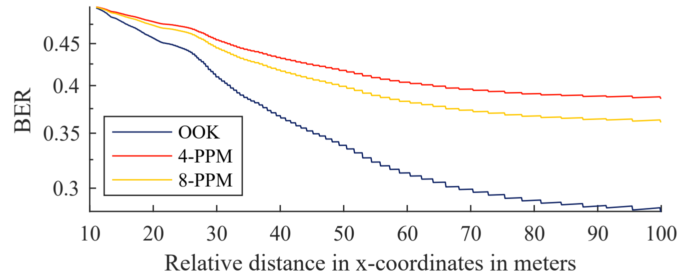

(a) BER curves for the HB over the distance

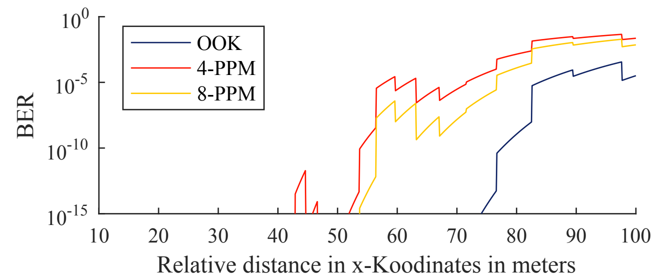

(b) BER curves for the HD84 headlight over the distance

Figure 9. BER curves.

we look at the achievable RSS, the interference power, and the BER under the presence of noise and multiuser interference. The scenario is simulated with the HB as a reference and with the HD84 system, while for the HD84 at every position the optimal LED is chosen, as shown in Figure 7. Since the LB has wide areas with low signal strength it is not further considered in this evaluation.

1) Signal and Interference Power in a Dynamic Two Lane Scenario: In Figure 8, we plot the signal power at RX1 and the interference power at RX2 over the distance x. It can be seen that the interference of the high beam is even higher than its signal. This is due to the fact that there is no way to control the direction of the signal at the high beam and, therefore, more signal is radiated to the center (RX2) than to the left lane (RX1). The difference between interference power and signal power is relatively small. Thus, even if we would swap the roles of RX1 and RX2, there would still be high interference.

In contrast, if we look at the HD84 matrix light, we control the LED by choosing the optimal LED at each situation (cf. Figure 7). Therefore, we can achieve a high signal power which is comparable to the signal strength of the HB at the center, even at the left lane. Because the signal is only radiated into a small area, the interference is reduced to a minimum. Now, the interference can be neglected in comparison to the effect of noise, which in this scenario has a power of −58.893 dBm.

2) Bit Error Ratio in a Dynamic Two Lane Scenario: The noise consists of thermal noise and shot noise. As the thermal noise ($\sigma_{thermal}$) we assume the noise given in the data sheet of the Photodiode Thorlabs PDA100a (cf. Table I). For other receiver circuits, the thermal noise can be calculated as

$$\sigma^2_{thermal} = \frac{4k_B T}{R_L} B F_n \ , \tag{8}$$

with k_B the Boltzman constant, T the temperature, R_L the load resistance, and F_n the noise figure. The shot noise (σ_{shot}) is given by [20] as

$$\sigma^2_{shot} = 2qB(RP_r + I_{dark}) \ , \tag{9}$$

with B the receiver bandwidth, R the responsivity of the PD, P_r the received power, and I_{dark} the dark current, which consists of the current introduced by the illumination of the sun in this case. For the interference power I, we assume that both transmitting cars are transmitting with the full power of the corresponding light module continuously in the whole frequency band. To calculate the BER, first the Signal-to-Interference-and-Noise Ratio (SINR) is calculated, consisting of the signal power S divided by the sum of thermal noise $\sigma_{thermal}$, shot noise σ_{shot}, and the interference power I:

$$SINR = \frac{S}{\sigma_{thermal} + \sigma_{shot} + I} \ . \tag{10}$$

In the following, we assume the interference as white Gaussian noise in the frequency band of interest. The BER for Non-Return-to-Zero-On-Off Keying (NRZ-OOK) modulation can be calculated as

$$BER_{NRZ-OOK} = \frac{1}{2} \operatorname{erfc}\left(\frac{\sqrt{SINR}}{2\sqrt{2}}\right) \ , \tag{11}$$

where erfc is the error function. For Pulse Position Modulation (L-PPM), the equation is

$$BER_{L-PPM} = \frac{1}{2} \operatorname{erfc}\left(\frac{\sqrt{SINR \frac{L}{2} \log_2 L}}{2\sqrt{2}}\right) \ , \tag{12}$$

with L the modulation order of the L-PPM.

In Figure 9a, we show the BER of the HB. Due to the high interference, no reliable transmission is possible. The BER decreases because the signal power is decreasing less than the interference power as it is shown in Figure 8, but still stays at a value that does not permit any useful communication. In Figure 9b, we show the BER of the HD84. The communication is much more reliable due to the very small interference power. For small distances, the BER is very small because the signal is very strong while noise and interference are low. For larger distances, the signal power decreases following the inverse square law, while the noise introduced by the receiver circuits stays constant. Therefore, the SINR decreases and the BER increases. With an error rate of less than 10^{-6}, it is possible to communicate with OOK for up to 60 m.

The strong fluctuations of the curves in Figure 9b are caused by the following effects. First, the logarithmic scale in a region of very small values make differences appear rather large, even if they are not relevant in a real implementation. Second, the fluctuations with a longer period are caused by switching between the LEDs. The same effect can me observed in Figure 8 but less significant. If this influences the communication negativity, also the neighboring LEDs could be modulated. Third, the optical simulation was run with a relatively low resolution of $0.2°$ to be more accurate in the regions of low power. This causes the stair-like shape. Note that, we consider the first stage of noise which consists of shot and thermal noise of the photo diode and the trans-impedance amplifier. Further stages like an Analog-to-Digital Converter (ADC) will introduce additional noise, which depends strongly to the choice of hardware and therefore is not included in the simulation. These effects can be compensated by special hardware design, applying coding and optical amplification. With these methods further distances and higher order modulation can be achieved.

VI. Conclusion

We proposed a novel SDMA approach to reduce multiuser interference for V-VLC by taking advantage of modern matrix LED-based AFS. Our system selects the LED for best communication performance from a matrix of LEDs in a headlight. Results show that this approach significantly reduces interference below the noise level, without the need for additional multiple access techniques. Therefore, valuable communication resources like bandwidth or time can be saved, while data rate and latency can be improved in comparison to systems which rely exclusively on traditional multiple access techniques (e.g., TDMA, CDMA, or FDMA.)

In future work, we plan to validate the system with outdoor measurements. Moreover, we plan to improve the system with receiver-based solutions. Additionally, optical elements can be used to further increase the signal strength while keeping the thermal noise constant, therefore decreasing the BER.

VII. Acknowledgements

The authors would like to thank HELLA GmbH & Co. KGaA and all colleagues involved for their support.

References

[1] ETSI, "Intelligent Transport Systems (ITS); Framework for Public Mobile Networks in Cooperative ITS (C-ITS)," ETSI, TR 102962 V1.1.1, Feb. 2012.

[2] C. Sommer and F. Dressler, *Vehicular Networking*. Cambridge University Press, 2014.

[3] IEEE, "Wireless Access in Vehicular Environments," IEEE, Std 802.11p-2010, Jul. 2010.

[4] M. Gonzalez-Martín, M. Sepulcre, R. Molina-Masegosa, and J. Gozalvez, "Analytical Models of the Performance of C-V2X Mode 4 Vehicular Communications," *IEEE Transactions on Vehicular Technology*, vol. 68, no. 2, pp. 1155–1166, Feb. 2019.

[5] A. Memedi, C. Sommer, and F. Dressler, "On the Need for Coordinated Access Control for Vehicular Visible Light Communication," in *IEEE/IFIP WONS 2018*, Isola 2000, France: IEEE, Feb. 2018, pp. 121–124.

[6] M. Boban, A. Kousaridas, K. Manolakis, J. Eichinger, and W. Xu, "Connected Roads of the Future: Use Cases, Requirements, and Design Considerations for Vehicle-to-Everything Communications," *IEEE Vehicular Technology Magazine*, vol. 13, no. 3, pp. 110–123, Sep. 2018.

[7] A.-M. Cailean and M. Dimian, "Current Challenges for Visible Light Communications Usage in Vehicle Applications: A Survey," *IEEE Communications Surveys & Tutorials*, vol. 4, no. 19, pp. 2681–2703, 2017.

[8] H.-Y. Tseng, Y.-L. Wei, A.-L. Chen, H.-P. Wu, H. Hsu, and H.-M. Tsai, "Characterizing link asymmetry in vehicle-to-vehicle Visible Light Communications," in *IEEE VNC 2015*, Kyoto, Japan: IEEE, Dec. 2015, pp. 88–95.

[9] "Uniform Provisions Concerning the Approval of Motor Vehicle Headlamps Emitting an Asymmetrical Passing Beam or a Driving Beam or Both and Equipped with Filament Lamps," United Nations, Tech. Rep. Regulation No. 112 - Revision 1, Oct. 2006.

[10] A. Memedi, H.-M. Tsai, and F. Dressler, "Impact of Realistic Light Radiation Pattern on Vehicular Visible Light Communication," in *IEEE GLOBECOM 2017*, Singapore, Singapore: IEEE, Dec. 2017.

[11] A. Memedi, C. Tebruegge, J. Jahneke, and F. Dressler, "Impact of Vehicle Type and Headlight Characteristics on Vehicular VLC Performance," in *IEEE VNC 2018*, Taipei, Taiwan: IEEE, Dec. 2018.

[12] P. Luo, Z. Ghassemlooy, H. L. Minh, E. Bentley, A. Burton, and X. Tang, "Bit-error-rate performance of a car-to-car vlc system using 2×2 mimo," *The Mediterranean Journal of Computers and Networks (MEDJCN)*, vol. 11, no. 2, pp. 400–407, Apr. 2015.

[13] B. Turan, S. Ucar, S. Coleri Ergen, and O. Ozkasap, "Dual Channel Visible Light Communications for Enhanced Vehicular Connectivity," in *IEEE VNC 2015*, Kyoto, Japan: IEEE, Dec. 2015, pp. 84–87.

[14] O. Narmanlioglu, B. Turan, S. Coleri Ergen, and M. Uysal, "Cooperative MIMO-OFDM based inter-vehicular visible light communication using brake lights," *Elsevier Computer Communications*, vol. 120, no. C, pp. 138–146, May 2018.

[15] A. Ashok, M. Gruteser, N. Mandayam, J. Silva, M. Varga, and K. Dana, "Challenge : Mobile Optical Networks Through Visual MIMO," in *ACM MobiCom 2010*, Chicago, IL: IEEE, Sep. 2010.

[16] I. Takai, T. Harada, M. Andoh, K. Yasutomi, K. Kagawa, and S. Kawahito, "Optical Vehicle-to-Vehicle Communication System Using LED Transmitter and Camera Receiver," *IEEE Photonics Journal*, vol. 6, no. 5, pp. 1–14, Oct. 2014.

[17] Y. Goto, I. Takai, T. Yamazato, H. Okada, T. Fujii, S. Kawahito, S. Arai, T. Yendo, and K. Kamakura, "A New Automotive VLC System Using Optical Communication Image Sensor," *IEEE Photonics Journal*, vol. 8, no. 3, pp. 1–17, Jun. 2016.

[18] P. Luo, M. Zhang, Z. Ghassemlooy, H. Le Minh, H. M. Tsai, X. Tang, L. C. Png, and D. Han, "Experimental Demonstration of RGB LED-Based Optical Camera Communications," *IEEE Photonics Journal*, vol. 7, no. 5, Oct. 2015.

[19] C. Tebruegge, Q. Zhang, and F. Dressler, "Optical Interference Reduction with Spatial Filtering Receiver for Vehicular Visible Light Communication," in *IEEE ITSC 2019*, Auckland, New Zealand: IEEE, Oct. 2019.

[20] T. Komine and M. Nakagawa, "Fundamental analysis for visible-light communication system using LED lights," *Consumer Electronics, IEEE Transactions on*, vol. 50, no. 1, pp. 100–107, Feb. 2004.